Electronic Supplementary Information

Experimental Section

Materials: Iron nitrate ($Fe(NO_3)_3 \cdot 9H_2O$), cobalt nitrate ($Co(NO_3)_2 \cdot 6H_2O$), Zinc acetate ($ZnAc_2$) and hexamethylenetetramine ($C_6H_{12}N_4$) were purchased from Beijing Chemical Corporation. RuO_2 particles were purchased from Sigma-Aldrich. Pt/C (20 wt%) was purchased from Alfa Aesar (China) Chemicals Co. Ltd. Potassium hydroxide (KOH), ethanol and Hydrochloric Acid (HCl) were purchased from Tianjing Chemical Corporation. Nafion (5 wt%) were purchased from Sigma-Aldrich Chemical Reagent Corporation. All reagents were used as received without further purification. Nickel foam (NF) was purchased from Phychemsi Hong Kong Company Limited and was cleaned by sonication sequentially in acetone, water and ethanol several times to remove the surface impurities. Ultrapure water was utilized to prepare all solutions.

Preparation of Fe-CoP/NF: Specifically, 1.0 mmol $Fe(NO_3)_3 \cdot 9H_2O$, 3.0 mmol $Co(NO_3)_2 \cdot 6H_2O$, 15 mmol $C_6H_{12}N_4$ were dissolved in 40 mL ultrapure water under magnetic stirring to form a uniform solution. The above solution and a piece of cleaned NF (2 cm × 3 cm) were transferred to a 50 mL Teflon-lined stainless-steel autoclave. The autoclave was sealed and placed in an oven at 100°C for 10 h and then cooled down naturally. The resulting product was taken out and washed with ultrapure water and dried at 60 °C for 12 hours. After that, the sample and NaH_2PO_2 were put at two separate positions in a porcelain boat with 1.0 g NaH_2PO_2 at the upstream side of the furnace. After added with Ar, the center of the furnace was elevated to 300 °C at a ramping rate of 2 °C min^{-1} and held at this temperature for 2 h, and then naturally cooled to ambient temperature under Ar. $Fe_{0.33}$-CoP/NF was converted from corresponding precursor. By diverse atomic ratio of the Fe:Co in solutions under other identical experimental conditions to get $Fe_{0.5}$-CoP/NF and $Fe_{0.2}$-CoP/NF. CoP/NF was made by using Co only. All experiments were carried out at room temperature (25 °C).

Preparation of ink catalysts and working electrode: 50 mg of $Fe_{0.33}$-CoP powder (scrape from $Fe_{0.33}$-CoP/NF) and 20 μL Nafion (5 wt%) solution were dispersed in 2.4 mL water/ethanol (V:V = 1:1) followed by 30 min sonication to form an ink. In addition, the same amount CoP, RuO_2 and Pt/C ink catalysts were also prepared for comparison and coated onto NF as the electrodes.

Characterizations: X-ray diffraction (XRD) measurements were performed using a RigakuD/MAX 2550 diffractometer with Cu Kα radiation (λ=1.5418 Å). Scanning electron microscopy (SEM) measurements were carried out on a XL 30 ESEM FEG scanning electron microscope at an accelerating voltage of 20 kV. Transmission electron microscopy (TEM) and High-resolution TEM (HRTEM) measurements were carried out on a Zeiss Libra 200 FE transmission electron microscope operated at 200 kV. X-ray photoelectron spectroscopy (XPS) measurements were performed on an ESCALABMK II X-ray photoelectron spectrometer using Mg as the exciting source. ICP analysis was performed on Thermo Scientific iCAP6300.

Electrochemical measurements: For ORR, all electrochemical measurements were performed with a CHI 660E electrochemical analyzer (CH Instruments, Inc., Shanghai) in a standard three-electrode system. The cyclic voltammetry (CV) experiments were performed in N_2- or O_2-staturated 0.1 M KOH at room temperature with a scan rate of 5 mV s^{-2}. The rotating disk electrode (RDE) tests were conducted in O_2-staturated 0.1 M KOH with a scan rate of 5 mV s^{-2}. Typically, The working electrodes were prepared by coating catalysts ink onto glassy carbon electrode (D = 5 mm) to form a catalyst film with a loading amount of about 1.65 mg cm^{-2}, Pt wire and Hg/HgO were used as counter electrode and reference electrode, respectively. To ensure the O_2/H_2O equilibrium, a flow of O_2 was maintained into the electrolyte during the entire ORR process.

OER and HER test were conducted in a standard three-electrode system using $Fe_{0.33}$-CoP/NF as the working electrode, a graphite rod as the counter electrode and an Hg/HgO electrode as the reference electrode. The RuO_2 and Pt/C electrode were prepared by coated the catalysts ink on NF to achieve 1.65 mg cm^{-2} of catalyst loading. The potentials in this work were calibrated to reversible hydrogen electrode

(RHE), using the following equation: E (RHE) = E (Hg/HgO) + (0.098 + 0.059 pH) V. Polarization curves were obtained using linear sweep voltammetry with a scan rate of 5 mV s^{-1}, using a graphite rod as the counter electrode and an Hg/HgO as the reference electrode.

The zinc-air batteries (ZABs) were constructed with a polished Zn plate served as anode and the $Fe_{0.33}$-CoP/NF or CoP/NF as the air electrodes with a gas diffusion film on the air-facing side. The 6.0 M KOH and 0.2 M $ZnAc_2$ electrolyte was filled between the cathode and anode. For the Pt/C electrode, the catalyst ink (prepared above) was dropped on the NF to form uniform coating until achieved 1.65 mg cm^{-2} of catalyst loading.

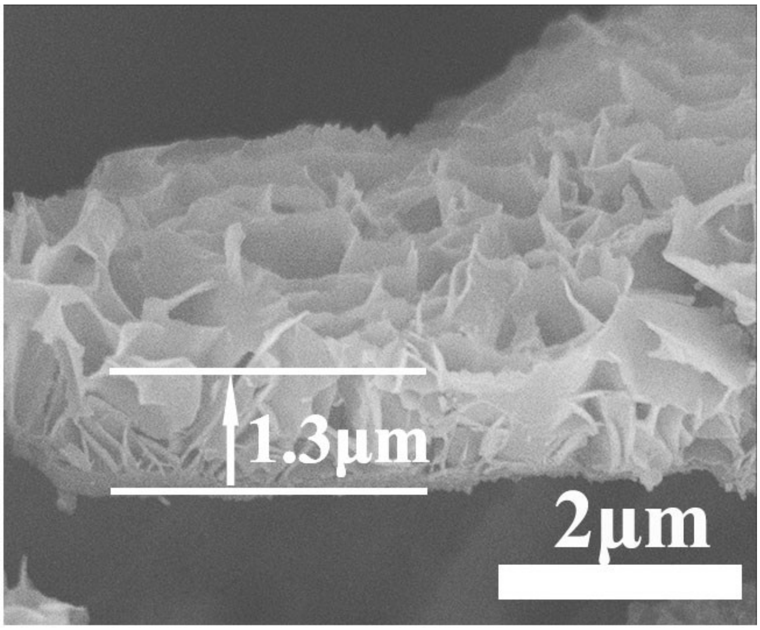

Fig. S1. Cross-section SEM image of $Fe_{0.33}$-CoP/NF.

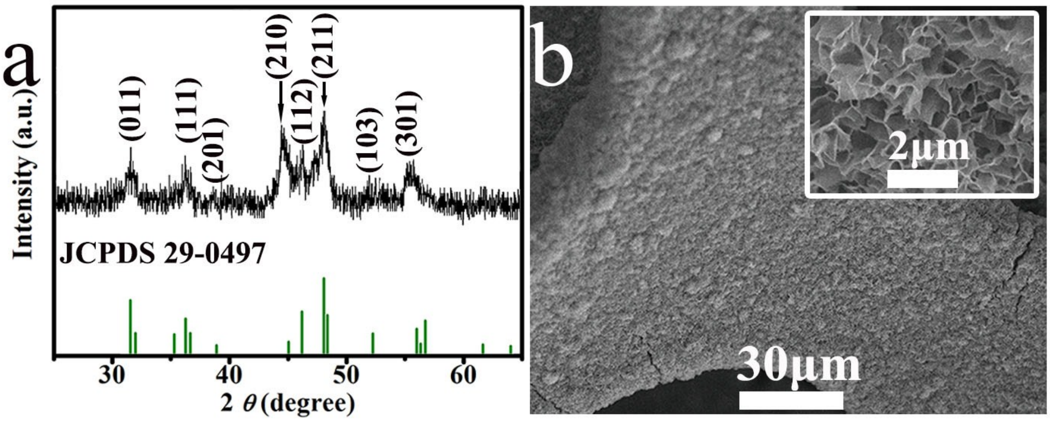

Fig. S2. (a) XRD pattern for CoP. (b) SEM images for CoP/NF.

.

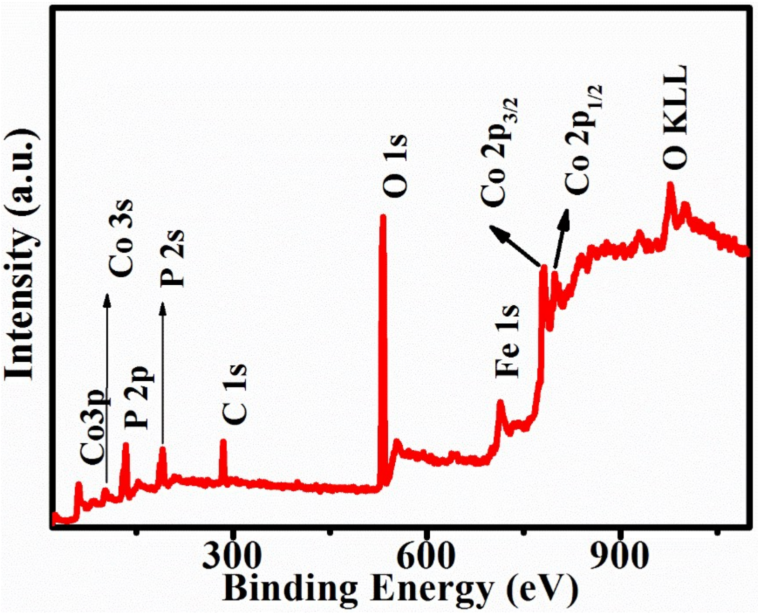

Fig. S3. XPS survey spectrum of $Fe_{0.33}$-CoP.

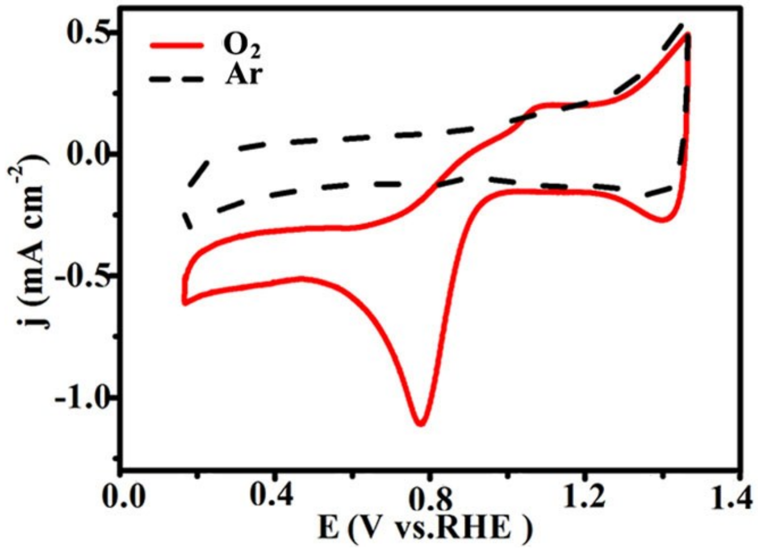

Fig. S4. CVs of $Fe_{0.33}$-CoP in an O_2- and Ar-saturated 0.1 M KOH with a scan rate of 5 mV s^{-1}.

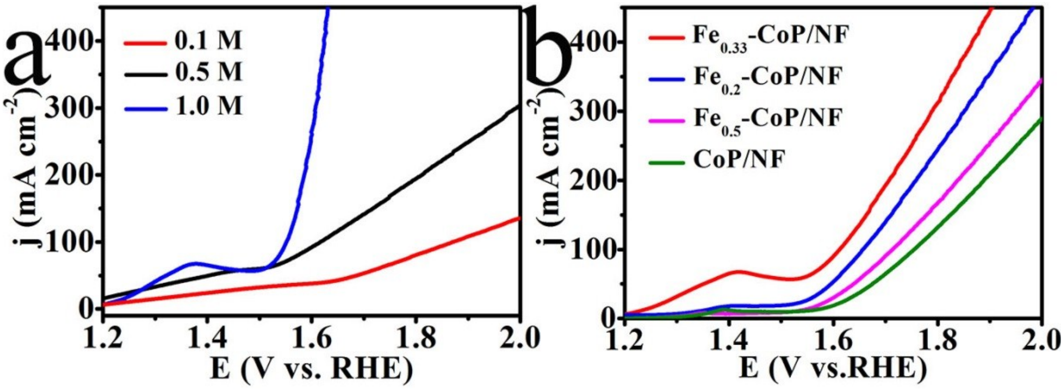

Fig. S5. (a) LSV curves of OER for $Fe_{0.33}$-CoP/NF in different electrolyte of 0.1 M, 0.5 M, and 1.0 M KOH with a scan rate of 5 mV s^{-1}. (b) LSV curves of OER for CoP/NF, $Fe_{0.33}$-CoP/NF, $Fe_{0.5}$-CoP/NF, and $Fe_{0.2}$-CoP/NF with a scan rate of 5 mV s^{-1} in 1.0 M KOH.

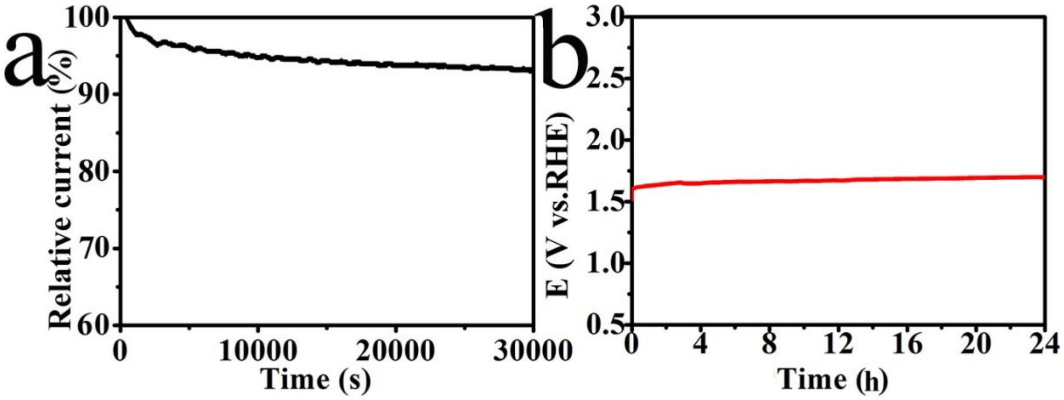

Fig. S6. (a) Time-dependent current density result of $Fe_{0.33}$-CoP/NF for ORR at 0.7 V in O_2-saturated 0.1 M KOH at 1600 rpm. (b) Chronopotentiometry result of $Fe_{0.33}$-CoP/NF for OER at a current density of 100 mA cm^{-2} in 1.0 M KOH.

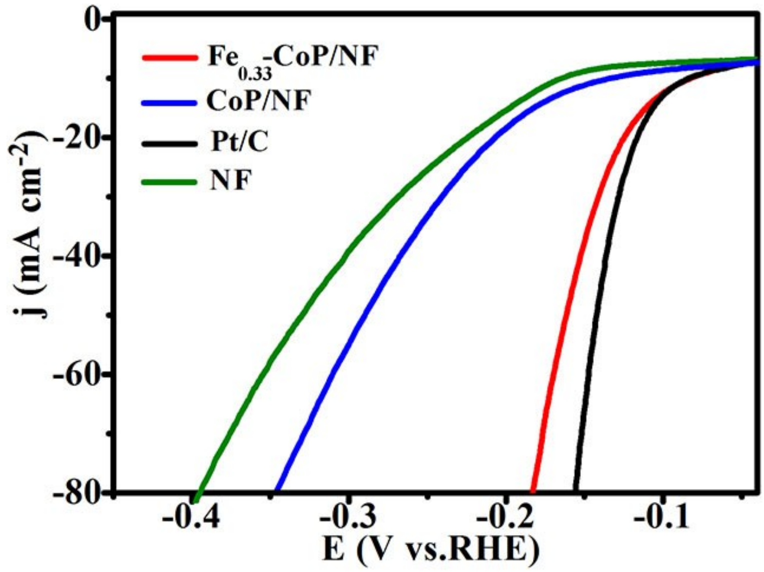

Fig. S7. LSV curves of HER for $Fe_{0.33}$-CoP/NF, CoP/NF, Pt/C on NF, and NF with a scan rate of 5 mV s^{-1} in 1.0 M KOH.

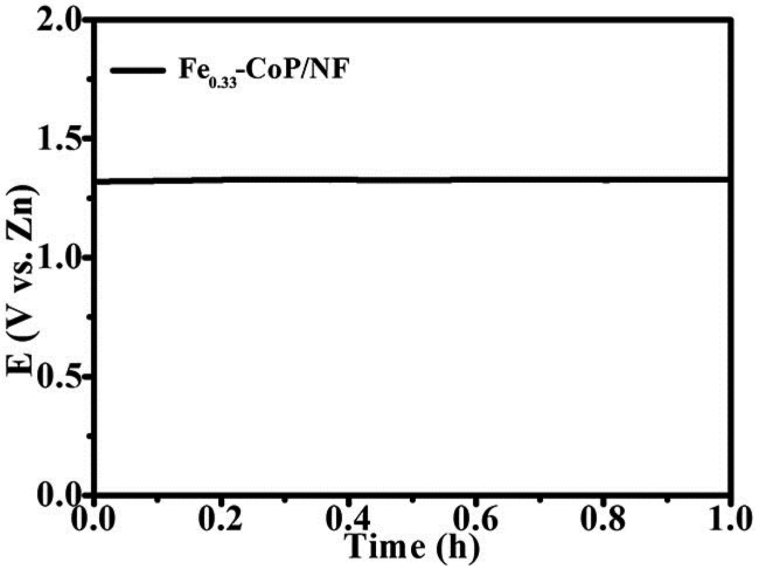

Fig. S8. Open circuit voltage measurement of one ZAB.

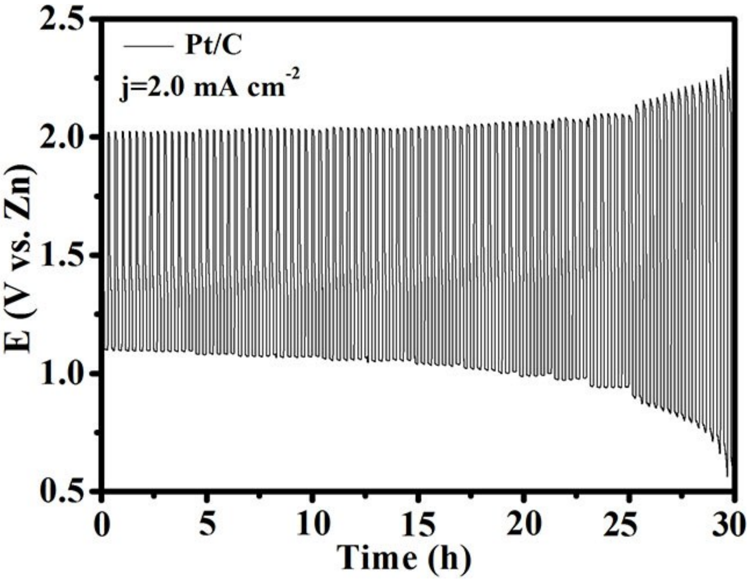

Fig. S9. long-term cycling tests of the ZAB using Pt/C on NF as the air cathode at the charging and discharging current density of 2.0 mA cm^{-2} (20 min for each cycle).

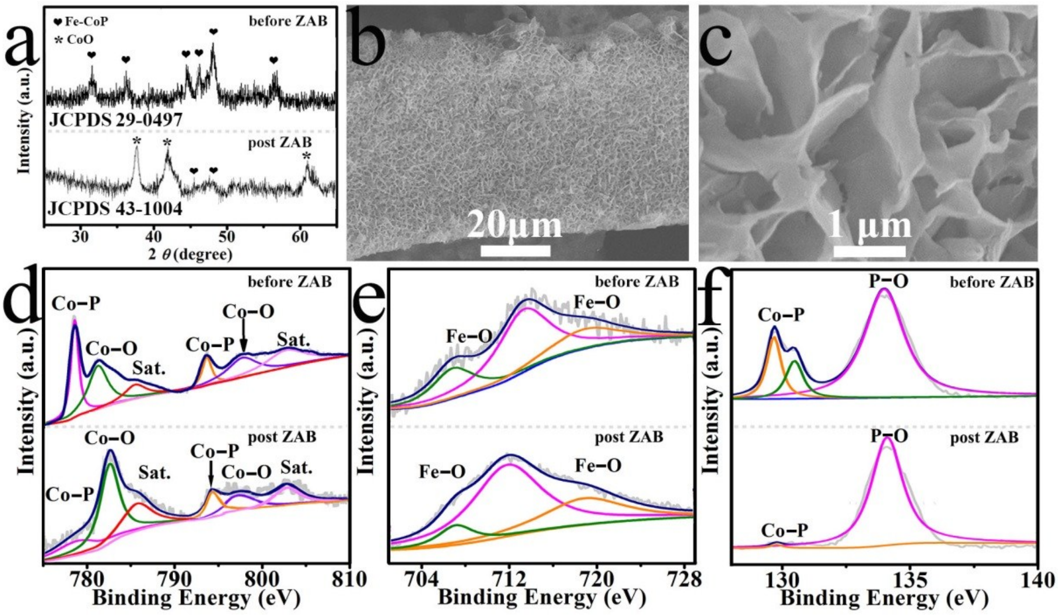

Fig. S10. Characterizations of the $Fe_{0.33}$-CoP/NF after the long time galvanostatic charge-discharge test serving as the electrode of ZAB. (a) XRD patterns and SEM images (b and c), (d-f) XPS spectra of Co, Fe, and P regions.

Table S1. Comparison of key performance parameters for ORR and rechargeable ZABs extracted from literature.

Catalysts	Half-wave potential (V vs. RHE)	Cycling time (h)	Electrolyte	Ref.
$Fe_{0.33}$-CoP/NF	0.80	200@20 mA cm^{-2}	0.1 M KOH	This work
$CoSb_3$	0.78	60@10 mA cm^{-2}	0.1 M KOH	1
FeCo@NC-750	0.80	20@10 mA cm^{-2}	0.1 M KOH	2
Co-PDA-C	0.77	16.7@2 mA cm^{-2}	0.1 M KOH	3
CoS_2(400)/N,S-GO	0.79	3.3@10 mA cm^{-2}	0.1 M KOH	4
CoNP@NC/ NG-700	0.78	100@5 mA cm^{-2}	0.1 M KOH	5
$NiCo_2O_4$-CNTs	0.80	40@10 mA cm^{-2}	0.1 M KOH	6
CoS_x@NS-GNs	0.72	50@1.25 mA cm^{-2}	0.1 M KOH	7
HCNT-Co_2P	0.76	-	0.1 M KOH	8
CoP@CC	0.67	10@10mA cm^{-2}	0.1 M KOH	9

Table S2. Comparison of key performance parameters for OER extracted from literature.

Catalysts	**j (mA cm^{-2})**	***η* (mV)**	**Electrolyte**	**Ref.**
$Fe_{0.33}$-CoP/NF	100	313	1.0 M KOH	This work
Fe-CoP-Pi-Bi/CC	10	382	1.0 M KOH	10
CoP/CN	10	300	1.0 M KOH	11
$Zn_{0.08}Co_{0.92}P$/TM	10	410	1.0 M KOH	12
CoP@PNC	10	330	1.0 M KOH	13
f-CoP/CoP_2/Al_2O_3	10	300	1.0 M KOH	14
CoP PNWs	10	326	1.0 M KOH	15
CoP/rGO-400	10	340	1.0 M KOH	16
Ni_2P-CoP	10	320	1.0 M KOH	17
Fe-CoP/Ti	100	310	1.0 M KOH	18
Co-NC@CoP-NC	10	330	1.0 M KOH	19

References

1 T. Yang, K. Zhou, G. Chen, W. Zhang and J. Liang, *RSC Adv.*, 2017, **7**, 33012–33019.

2 P. Cai, S. Ci, E. Zhang, P. Shao, C. Cao and Z. Wen, *Electrochim. Acta*, 2016, **220**, 354–362.

3 B. Li, Y. Chen, X. Ge, J. Chai, X. Zhang, T. S. Hor, G. Du, Z. Liu, H. Zhang and Y. Zong, *Nanoscale*, 2016, **8**, 5067–5075.

4 P. Ganesan, P. Ramakrishnan, M. Prabu and S. Shanmugam, *Electrochim. Acta*, 2015, **183**, 63–69.

5 X. Zhong, Y. Jiang, X. Chen, L. Wang, G. Zhuang, X. Li and J. Wang, *J. Mater. Chem. A*, 2016, **4**, 10575–10584.

6 C. Ma, N. Xu, J. Qiao, S. Jian and J. Zhang, *Int. J. Hydrogen Energy*, 2016, **41**, 9211–9218.

7 D. Geng, N. Ding, T. S. A. Hor, S. W. Chien, Z. Liu and Y. Zong, *RSC Adv.*, 2015, **5**, 7280–7284.

8 K. Chen, X. Huang, C. Wan and H. Liu, *RSC Adv.*, 2015, **5**, 92893–92895.

9 Y. Cheng, F. Liao, W. Shen, L. Liu, B. Jiang, Y. Li and M. Shao, *Nanoscale*, 2017, **9**, 18977–18982.

10 M. Ma, G. Zhu, F. Xie, F. Qu, Z. Liu, G. Du, A. M. Asiri, Y. Yao and X. Sun, *ChemSusChem*, 2017, **10**, 3188–3192.

11 B. Weng, W. Wei, Y. Wu, A. M. Alenizib and G. Zheng, *J. Mater. Chem. A*, 2016, **4**, 15353–15360.

12 T. Liu, D. Liu, F. Qu, D. Wang, L. Zhang, R. Ge, S. Hao, Y. Ma, G. Du, A. M. Asiri, L. Chen and X. Sun, *Adv. Energy Mater.*, 2017, **7**, 1700020.

13 Z. Zhou, N. Mahmood, Y. Zhang, L. Pan, L. Wang, X. Zhang and J. Zou, *J. Energy Chem.*, 2017, **26**, 1223–1230.

14 W. Li, S. Zhang, Q. Fan, F. Zhang and S. Xu, *Nanoscale*, 2017, **9**, 5677–5685.

15 M. Zhang, S. Ci, H. Li, P. Cai and H. Xu, *Int. J. Hydrogen Energy*, 2017, **42**,

29080–29090.

16 L. Jiao, Y. Zhou and H. Jiang, *Chem. Sci.*, 2016, **7**, 1690–1695.

17 X. Liang, B. Zheng, L. Chen, J. Zhang, Z. Zhuang and B. Chen, *ACS. Appl. Mater. Interfaces*, 2017, **9**, 23222–23229.

18 C. Tang, R. zhang, W. Lu, L. He, X. Jiang, A. M. Asiri and X. Sun, *Adv. Mater.*, 2017, **29**, 1602441.

19 X. Li, Q. Jiang, S. Dou, L. Deng, J. Huo and S. Wang, *J. Mater. Chem. A*, 2016, **4**, 15836–15840.